AD-A184 618 CURRENT-FILAMENTATION INSTABILITY IN RAILGUN ARCS(U) 1/1
ARMY BALLISTIC RESEARCH LAB ABERDEEN PROVING GROUND MD
J D POWELL JUN 87 BRL-MR-3613

UNCLASSIFIED F/G 20/9 NL

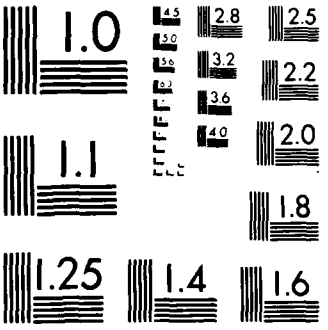

AD

MEMORANDUM REPORT BRL-MR-3613

CURRENT-FILAMENTATION INSTABILITY IN RAILGUN ARCS (U)

JOHN D. POWELL

JUNE 1987

US ARMY BALLISTIC RESEARCH LABORATORY
ABERDEEN PROVING GROUND, MARYLAND

Destroy this report when it is no longer needed.
Do not return it to the originator.

Additional copies of this report may be obtained from the National Technical Information Service, U. S. Department of Commerce, Springfield, Virginia 22161.

The findings in this report are not to be construed as an official Department of the Army position, unless so designated by other authorized documents.

The use of trade names or manufacturers' names in this report does not constitute indorsement of any commercial product.

UNCLASSIFIED
SECURITY CLASSIFICATION OF THIS PAGE

ADA184618

REPORT DOCUMENTATION PAGE

Form Approved
OMB No 0704-0188
Exp Date Jun 30, 1986

1a REPORT SECURITY CLASSIFICATION Unclassified	1b RESTRICTIVE MARKINGS
2a SECURITY CLASSIFICATION AUTHORITY NA	3 DISTRIBUTION/AVAILABILITY OF REPORT
2b DECLASSIFICATION/DOWNGRADING SCHEDULE	
4 PERFORMING ORGANIZATION REPORT NUMBER(S)	5 MONITORING ORGANIZATION REPORT NUMBER(S)
6a NAME OF PERFORMING ORGANIZATION US Army Ballistic Research Lab 6b OFFICE SYMBOL (If applicable) SLCBR-TB-EP	7a NAME OF MONITORING ORGANIZATION
6c ADDRESS (City, State, and ZIP Code) Aberdeen Proving Ground, MD 21005-5066	7b ADDRESS (City, State, and ZIP Code)
8a NAME OF FUNDING/SPONSORING ORGANIZATION US Army Ballistic Research Lab 8b OFFICE SYMBOL (If applicable) SLCBR-D	9 PROCUREMENT INSTRUMENT IDENTIFICATION NUMBER
8c ADDRESS (City, State, and ZIP Code) Aberdeen Proving Ground, MD 21005-5066	10 SOURCE OF FUNDING NUMBERS PROGRAM ELEMENT NO: 61102A PROJECT NO: AH43 TASK NO: 00 WORK UNIT ACCESSION NO: 001AJ

11 TITLE (Include Security Classification)

(U) Current-Filamentation Instability in Railgun Arcs

12 PERSONAL AUTHOR(S)
John D. Powell

13a TYPE OF REPORT	13b TIME COVERED FROM ____ TO ____	14 DATE OF REPORT (Year, Month, Day)	15 PAGE COUNT

16 SUPPLEMENTARY NOTATION

17 COSATI CODES			18 SUBJECT TERMS (Continue on reverse if necessary and identify by block number)
FIELD	GROUP	SUB-GROUP	Railgun arc, plasma instability, Rayleigh-Taylor instability, current-filamentation instability, electromagnetic propagation, plasma armature
20	09		

19 ABSTRACT (Continue on reverse if necessary and identify by block number) (idk)

We extend some previous analysis of Rayleigh-Taylor instabilities in railgun arcs to treat the current-filamentation instability. The basic model is similar to that used in our previous treatment of the interchange instability, and the formalism is adapted from that developed by Tsai, Liskow, and Wilcox. It is demonstrated that railgun arcs are indeed unstable to the formation of current filaments for any nonzero value of the acceleration. However, numerical solution of the appropriate eigenvalue problem suggests that the growth rates of the unstable modes are generally too small, and the wavelengths generally too large, for the instability to be of much practical importance.

20 DISTRIBUTION/AVAILABILITY OF ABSTRACT	21 ABSTRACT SECURITY CLASSIFICATION
☒ UNCLASSIFIED/UNLIMITED ☐ SAME AS RPT ☐ DTIC USERS	Unclassified
22a NAME OF RESPONSIBLE INDIVIDUAL John D. Powell	22b TELEPHONE (Include Area Code) (301) 278-5783
	22c OFFICE SYMBOL SLCBR-TB-EP

DD FORM 1473, 84 MAR — 83 APR edition may be used until exhausted. All other editions are obsolete.

SECURITY CLASSIFICATION OF THIS PAGE
UNCLASSIFIED

TABLE OF CONTENTS

I. INTRODUCTION

In a recent publication[1] we examined the susceptibility of railgun arcs to the Rayleigh-Taylor interchange instability. It was concluded that these plasmas were unstable and that the growth rates were usually large enough for effects of the instability to be seen in experiments of interest. In this report we will be interested in extending the previous analysis to another type of Rayleigh-Taylor effect, i.e., the current-filamentation instability. The two types of instability are differentiated according to the manner in which the initial steady state of the plasma is disturbed: In the interchange case, the perturbation wave vector lies in the same direction as the steady-state current; in the current-filamentation case, it lies along the same direction as the steady-state induction field.

The basic model and procedure will be the same as for our previous analysis. In particular, we will modify as needed the formalism worked out by Tsai, Liskow, and Wilcox (TLW)[2] to treat both types of instability in an accelerating plasma. These authors considered a plasma in which the conductivity varied linearly with the density, which had infinitely extended tails, and which was accelerated electromagnetically without a projectile. They concluded that the plasma was subject to both types of instability, with the interchange case having the larger growth rate. As pointed out in Ref. 1, however, it is more appropriate in railgun applications to assume constant conductivity for the arc. Under this assumption the arc becomes completely confined by the magnetic field and consideration must be given not only to differences in the solution of the plasma equations, but also to the boundary conditions that must hold at the interface between the plasma and the vacuum. In addition, both the steady-state and perturbed solutions are significantly affected by the projectile and its presence must be carefully accounted for.

The basic model to be used is shown in Fig. 1 and is identical to that assumed in Ref. 1. The upper and lower sides in the figure represent rails which carry current in the direction indicated. The current also flows through a plasma arc located in between $x = 0$ and $x = -\ell$. The entire current configuration produces a magnetic field which interacts with the arc current to produce, via the standard $\vec{J}\times\vec{B}$ force, a very high-pressure plasma. This plasma then accelerates the projectile (shaded area) down the gun tube. It has been shown[3] previously that the arc approaches a steady state in the accelerating frame of reference. In this calculation, as in our previous stability analysis, the steady state is subjected to perturbations in order to examine its subsequent behavior.

---

[1] *Powell, John D., "Interchange Instability in Railgun Arcs," Phys. Rev. A. 34, 3262 (1986). See also Ballistic Research Laboratory Report No. BRL-TR-2276, Jan 1987.*

[2] *Tsai, W., Liskow, D., and Wilcox, T., "Rayleigh-Taylor Instabilities of an Accelerating Thin Plasma," Phys. Fluids 24, 1676 (1981).*

[3] *Powell, John D. and Battek, Jad M., "Plasma Dynamics of an Arc-Driven, Electromagnetic, Projectile Accelerator," J. Appl. Phys. 52, 2717 (1981). See also "Plasma Dynamics of the Arc-Driven Rail Gun," Ballistic Research Laboratory Report No. ARBRL-TR-02167, Sep 1980.*

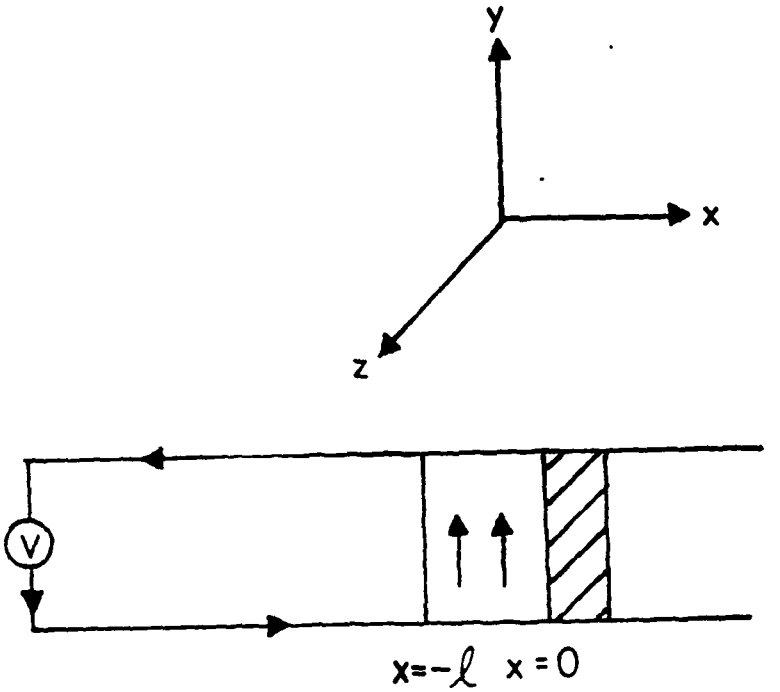

Figure 1. Model for stability calculations.

The assumptions indicated and discussed in Ref. 1 will also be made in this calculation: First, we will assume that the rails are perfect conductors and are infinitely extended in the z direction. Second, we will assume that the temperature within the arc is constant in both space and time. The spatial uniformity has been shown to be a fair assumption from our previous steady-state analysis, and temporal uniformity has been suggested as reasonable because of the extreme susceptibility of the arc to radiation. In general, temporally isothermal conditions can be expected to result if radiative losses rapidly smooth out temperature changes that would occur both because of Joule heating and because of local expansions and compressions within the arc. Finally, and most important, we neglect resistive effects in calculating the growth rates of the instabilities. In other words, finite conductivity is accounted for in obtaining the steady-state solution but, in the perturbation, the conductivity is assumed to be infinite. It is not known how reasonable this commonly made assumption is for railgun arcs and consideration of finite-conductivity effects is much needed. Some efforts underway to account for finite conductivity will be discussed in Sec. V.

The report is organized as follows. In Sec. II the basic formalism needed to carry out the calculation is presented. Much of this formalism is also contained in Ref. 2, but is indicated here as well in order to set the notation. In Sec. III the calculation is carried through. In Sec. IV the results are discussed, compared with the results of TLW, and compared with the results for the interchange instability.

II. FORMALISM

We choose the origin of the coordinate system to be located at the back of the projectile and to move with it. All quantities calculated are those measured by an observer in the accelerating reference frame. Let ρ, P and $\vec{v}$ be the density, pressure and velocity in the arc. Let $\vec{E}$, $\vec{B}$ and $\vec{J}$ be the electric-field intensity, the magnetic-induction field, and the current density. Let σ be the conductivity and a the acceleration. We then assume that the arc is governed by the standard magnetohydrodynamic equations:

$$\frac{\partial \rho}{\partial t} + \vec{\nabla} \cdot (\rho \vec{v}) = 0 \tag{1}$$

$$\rho \frac{\partial \vec{v}}{\partial t} + \rho \vec{v} \cdot \vec{\nabla} \vec{v} + \vec{\nabla} P = \vec{J} \times \vec{B} - \rho \vec{a} \tag{2}$$

$$\vec{\nabla} \times \vec{E} = - \frac{\partial \vec{B}}{\partial t} \tag{3}$$

$$\vec{\nabla} \times \vec{B} = \mu \vec{J} , \quad \vec{\nabla} \cdot \vec{B} = 0 \tag{4}$$

$$\vec{J} = \sigma(\vec{E} + \vec{v} \times \vec{B}) \tag{5}$$

and

$$P = \frac{(1 + \alpha)}{M_0} k_B T \rho = K \rho \quad . \tag{6}$$

Equations (1) and (2) express mass and momentum conservation; Eqs. (3) and (4) are Maxwell equations; Eq. (5) is Ohm's law; and Eq. (6) is the isothermal equation of state. In Eq. (6) α represents the ratio of electrons to heavy particles in the plasma, k_B is Boltzmann's constant, T is the temperature, and M_0 is the ion (or neutral) mass. Physically, K represents the square of the acoustical propagation velocity in the plasma under isothermal conditions. In Eq. (4) μ is the free-space permeability.

As shown in Ref. 1 Eqs. (2)-(6) can be partially uncoupled to produce expressions for $\vec{B}$ and $\vec{v}$. One finds

$$\frac{\partial \vec{B}}{\partial t} = \vec{\nabla} \times (\vec{v} \times \vec{B}) + \frac{1}{\mu \sigma} \left[\frac{\vec{\nabla} \sigma}{\sigma} \times (\vec{\nabla} \times \vec{B}) + \nabla^2 \vec{B} \right] \tag{7}$$

and

$$\rho \frac{\partial \vec{v}}{\partial t} + \rho \vec{v} \cdot \vec{\nabla} \vec{v} + K \vec{\nabla} \rho = \frac{1}{\mu} [(\vec{B} \cdot \vec{\nabla}) \vec{B} - \tfrac{1}{2} \vec{\nabla} B^2] - \rho \vec{a} \quad . \tag{8}$$

Consequently, Eqs. (1), (7) and (8) can be solved to determine ρ, $\vec{B}$ and $\vec{v}$, and the remaining plasma variables determined from Eqs. (1)-(6).

According to the standard procedure used in stability analysis, we assume that the solution to Eq. (1), (7) and (8) can be represented by the steady-state solution plus a small time-dependent correction, i.e., for each function $\vec{F}$

$$\vec{F}(\vec{x},t) = \vec{F}_0(x) + \vec{F}_1(\vec{x},t) \quad . \tag{9}$$

Furthermore for the current-filamentation instability, the spatial and time dependence of each $\vec{F}_1$ is assumed to be of the form

$$\vec{F}_1(\vec{x},t) = \hat{\vec{F}}_1(x)e^{i(kz - \omega t)} = \hat{\vec{F}}_1(x)\, e^{i\phi} \quad . \tag{10}$$

Here $\vec{k} = k\hat{a}_z$ is the perturbation wave number and ω the angular frequency. For any given real value of k, ω must be determined from the calculation. If, then, $\mathrm{Im}(\omega) > 0$, the perturbation grows in time and the plasma is unstable. The assumption that the perturbation wave number has only a z component (lies along the direction of the unperturbed $\vec{B}$ field) should be contrasted with the interchange instability treated previously, in which $\vec{k}$ was assumed to have only a y component (be along the direction of the unperturbed current).

The equations that must be obeyed in the steady state are obtained by substituting Eq. (9) into Eqs. (1), (7) and (8), retaining only the lowest-order terms, and noting that $\vec{v} = 0$ in the steady state. One finds

$$\frac{d^2B_0}{dx^2} = \frac{1}{c_0}\frac{dc_0}{dx}\frac{dB_0}{dx} \tag{11}$$

and

$$K\frac{dc_0}{dx} = -\frac{B_0}{\mu}\frac{dB_0}{dx} - c_0 a_0 \tag{12}$$

Similarly, the first-order equations are obtained by substituting Eq. (9), with each $\vec{F}_1$ represented by Eq. (10), into Eqs. (1), (7) and (8) and retaining only the first-order terms. The following equations then result:

$$-i\omega\rho_1 + (\rho_0 v_{1x})' + i k \rho_0 v_{1z} = 0 \tag{13}$$

$$\omega B_{1x} = -k B_0 v_{1x} \tag{14}$$

$$i\omega B_{1x} = (B_0 v_{1x})' \tag{15}$$

$$i\omega\rho_0 v_{1x} = K\rho_1' + \frac{B_0}{\mu} B_{1z}' + \frac{B_{1z}}{\mu} B_0' - \frac{ik}{\mu} B_0 B_{1x} + \rho_1 a_0 \tag{16}$$

$$i\omega\rho_0 v_{1z} = i\,k\,K\,\rho_1 - \frac{B_{1x}}{\mu} B_0' \tag{17}$$

where the primes denote differentiation with respect to x. The expressions for B_{1y} and v_{1y} are not included since they do not affect the dispersion relation. These variables can therefore be set equal to zero without any loss of generality.

Equations (13)-(17) can be simplified so that all plasma variables are expressed in terms of v_{1x} by the following operations. We first substitute Eq. (14) into Eq. (17) and the result into Eq. (13) to produce

$$i\omega\rho_1 = \frac{1}{\omega^2 - k^2K} \left[\omega^2(\rho_0 v_{1x})' + \frac{k^2 B_0}{\mu} B_0' v_{1x}\right] . \tag{18}$$

Similarly, we substitue Eq. (14) into Eq. (17) and Eq. (18) into the result to yield

$$ik\rho_0 v_{1z} = \frac{k^2}{\omega^2 - k^2K}\left[K(\rho_0 v_{1x})' + \frac{B_0}{\mu} B_0' v_{1x}\right] . \tag{19}$$

Finally, a single, second-order differential equation for v_{1x} can be obtained by using Eqs. (19), (15) and (14) in Eq. (16). The result is

$$A_1 v_{1x}'' + A_2 v_{1x}' + A_3 v_{1x} = 0 \tag{20}$$

where

$$A_1 = \frac{B^2_0}{\mu K \rho_0} + \gamma$$

$$A_2 = \left(\frac{a_0}{K} + \frac{2\rho_0'}{\rho_0}\right)\gamma + \frac{B_0}{\mu K \rho_0} B_0' (2 + \gamma) \tag{21}$$

and

$$A_3 = \frac{1}{K}\left(\omega^2 - \frac{k^2 B_0^2}{\mu\rho_0}\right) + \frac{a_0 k^2}{\omega^2 - k^2 K} \frac{B_0}{\mu K \rho_0} B_0'$$

and γ is given by

$$\gamma = \frac{\omega^2}{\omega^2 - k^2 K} . \tag{22}$$

Evidently, then, once Eq. (20) has been solved for v_{1x}, results for ρ_1, v_{1z}, B_{1x} and B_{1z} follow from Eqs. (18), (19), (14) and (15), respectively.

We next observe that Eqs. (1)-(6) hold not only in the plasma but in the vacuum as well with $\rho = 0$ and $\sigma = 0$. They therefore imply certain boundary conditions that must hold at the interface between the plasma and the vacuum if, as in the case considered here, the plasma is completely confined by the magnetic field. These boundary conditions have been derived for a general case by Kruskal and Schwartzschild.[4] For the case at hand we have

$$\hat{n} \cdot [\vec{B}] = 0 \tag{23}$$

$$\mu \vec{j}^* = \hat{n} \times [\vec{B}] \tag{24}$$

$$\hat{n} \times [\vec{E}] = (\hat{n} \cdot \vec{v})[\vec{B}] \tag{25}$$

$$[K\rho + \frac{B^2}{2\mu}] = 0 \quad . \tag{26}$$

Here $\hat{n}$ represents the unit normal to the separating surface (pointing toward the plasma) and the brackets denote the change in the quantity in question as the interface is crossed. The parameter $\vec{j}^*$ represents the surface current. These conditions are necessary to yield the value of the derivative of v_{1x} at $x = -\ell_0$, needed to solve Eq. (20) numerically as well as to join the vacuum fields to those in the plasma.

III. CALCULATIONS

In the previous section the formalism needed to determine the susceptibility of the arc to the current-filamentation instability was presented. In this section the calculation is actually carried through.

In Ref. 1 the solution of the steady-state equations, i.e., Eqs. (11) and (12) was obtained for σ = constant. We found

$$\vec{B}_0 = -\mu j \, x/\ell_0 \, \hat{a}_z \quad , \quad -\ell_0 \leq x \leq 0 \tag{27}$$

$$\vec{B}_0 = \mu j \, \hat{a}_z \quad , \quad -\infty < x < -\ell_0$$

and

$$\rho_0 = \frac{2(1+\beta)\rho_\ell}{\beta \chi \ell_0} \left[1 - \chi \frac{x}{\ell_0} - (1+\chi)e^{-\chi(1+x/\ell_0)}\right] \quad . \tag{28}$$

---

[4] Kruskal, M. and Schwartzschild, M., "Some Instabilities of a Completely Ionized Plasma," Proc. R. Soc. London Ser. A 223, 348 (1954).

In these equations, j represents the current per unit height on the rail surface, ℓ_0 is the steady-state length of the arc, β is the ratio of the arc-to-projectile mass, and ρ_ℓ is the area density of the arc. The parameter χ is given explicitly by

$$\chi = \frac{\mu j^2 \beta \ell_0}{2K\rho_\ell(1+\beta)} = \frac{a_0 \ell_0}{K} \quad , \tag{29}$$

and must satisfy the transcendental equation

$$1 = \frac{2(1+\beta)}{\beta\,\chi} \left[1 + \chi/2 - \frac{1+\chi}{\chi}(1-e^{-\chi})\right] \quad . \tag{30}$$

The constraint imposed by Eq. (30) determines the unperturbed arc length ℓ_0.

We now proceed to determine the electromagnetic fields within the vacuum to the left of the plasma. These fields are necessary to match the boundary conditions implied by Eqs. (23)-(26). In the vacuum we have for the first-order fields

$$\vec{\nabla} \times \vec{B}_1^V = 0 \quad , \quad \vec{\nabla} \cdot \vec{B}_1^V = 0 \tag{31}$$

$$\vec{\nabla} \times \vec{E}_1^V = -\frac{\partial \vec{B}_1^V}{\partial t} \quad , \quad \vec{\nabla} \cdot \vec{E}_1^V = 0 \quad . \tag{32}$$

The superscript V has been attached to differentiate the vacuum fields from those in the plasma. If we make the assumption that the spatial and time dependence of these first-order quantities is as given in Eq. (9), Eqs. (31) and (32) are easily solved to yield*

$$\begin{aligned} B_{1x}^V &= \tilde{B}_{1x}^V \, e^{k(x+\ell_0)} \, e^{i\phi} \\ B_{1y}^V &= 0 \\ B_{1z}^V &= i \, \tilde{B}_{1x}^V \, e^{k(x+\ell_0)} \, e^{i\phi} \quad . \end{aligned} \tag{33}$$

and

*We consider only the case $k > 0$. It can be shown that the resulting dispersion relations, discussed subsequently in Figs 2 and 3, depend only on $|k|$.

$$E_{1x}^V = \tilde{E}_{1x}^V \, e^{k(x+\ell_0)} e^{i\phi}$$

$$E_{1y}^V = - \omega/k \, \tilde{B}_{1x}^V \, e^{k(x+\ell_0)} e^{i\phi} \qquad (34)$$

$$E_{1z}^V = i \, \tilde{E}_{1x} e^{k(x+\ell_0)} e^{i\phi} \quad .$$

In these equations $\tilde{B}_{1x}^V$ and $\tilde{E}_{1x}^V$ are constants which must be determined from the boundary conditions.

In the steady state the equation of the surface which separates the plasma and the vacuum is given by $x = -\ell_0$ and the unit normal to the surface is simply $\hat{n}_0 = \hat{a}_x$. In the perturbed configuration, the equation of the surface is

$$x = - \ell_0 + \delta_x(z,t) \qquad (35)$$

where δ_x is given to first order by

$$\delta_x(z,t) = \frac{iv_0}{\omega} e^{i\phi} \qquad (36)$$

and where $v_0 = v_{1x}$ $(x = -\ell_0)$. Consequently, in the perturbed state the unit normal to the interface is, to first order, given by

$$\hat{n} = \hat{a}_x + \frac{v_0 k}{\omega} e^{i\phi} \hat{a}_z \quad . \qquad (37)$$

We finally observe that for zeroth- and first-order quantities $\vec{F}_0$ and $\vec{F}_1$, we have through terms of first-order

$$\vec{F}_1(-\ell_0 + \delta_x) = \vec{F}_1(-\ell_0)$$

and (38)

$$\vec{F}_0(-\ell_0 + \delta_x) = \vec{F}_0(-\ell_0) + \left(\frac{\partial \vec{F}_0}{\partial x}\right)_{x = -\ell_0} \delta_x \, .$$

We now use the results of Eqs. (36)-(38), the plasma equations [Eqs. (18), (19), (14) and (15)], and the steady-state results [Eqs. (27) and (28)] to satisfy the boundary conditions represented by Eqs. (23)-(26). One finds after algebra that these conditions imply the following results:

$$\tilde{B}^{V}_{1x} = - \frac{k\mu j v_0}{\omega}$$

$$\tilde{J}^{*}_{1} = 0 \qquad (39)$$

$$v_0' = k\, v_0$$

and

$$\tilde{E}^{V}_{1x} = 0$$

where v_0' means the derivative of v_{1x} at $x = - \ell_0$. Evidently all constants have now been expressed in terms of v_0 and the derivative v_0', necessary to solve Eq. (20) has been obtained.

It remains now only to solve Eq. (20). In addition to the condition on v_{1x} at $x = - \ell_0$, it is apparent that v_{1x} must also satisfy the condition

$$v_{1x}(x = 0) = 0, \qquad (40)$$

i.e., the plasma velocity (in the moving reference frame) must vanish at the projectile surface. For any given value of k, this condition can be satisfied only for certain discrete values of ω^2 and, if any of these is negative, the corresponding mode and hence the plasma is unstable.

Our procedure for solving Eq. (20) has been to assume values of k^2 and vary ω^2 until the boundary condition set forth in Eq. (40) was satisfied. By continuing this procedure for various values of k^2, the dispersion curve, ω versus k, can be computed. Prior to carrying out the numerical integration we have expressed the coefficients in Eq. (21) in terms of dimensionless quantities

$$\bar{B}_0 = \frac{B_0}{\mu j}\ ,\ \bar{\rho}_0 = \frac{\ell_0 \rho_0}{\rho_\ell}\ ,\ \bar{k} = k\ell_0, \text{ and } \bar{\omega} = \frac{\omega \ell_0}{\sqrt{K}}\ .$$

We have also made the transformation $z = 1 + x/\ell_0$ which maps the interval $(-\ell_0, 0)$ into $(0,1)$. It is then found that the dispersion curve for the dimensionless variables, $\bar{\omega}$ versus $\bar{k}$, depends only on β.

The numerical integration has been carried out for a wide range of values of β. Typical of the results obtained are those shown in Fig. 2 in which $|\omega|/\chi$ is plotted versus $|k|/\chi$ for $\beta = 0.05$, 0.1 and 0.5, and in Fig. 3 for $\beta = 1.0$, 3.0 and 5.0. These curves constitute the central result of our calculation and are discussed in the following section.

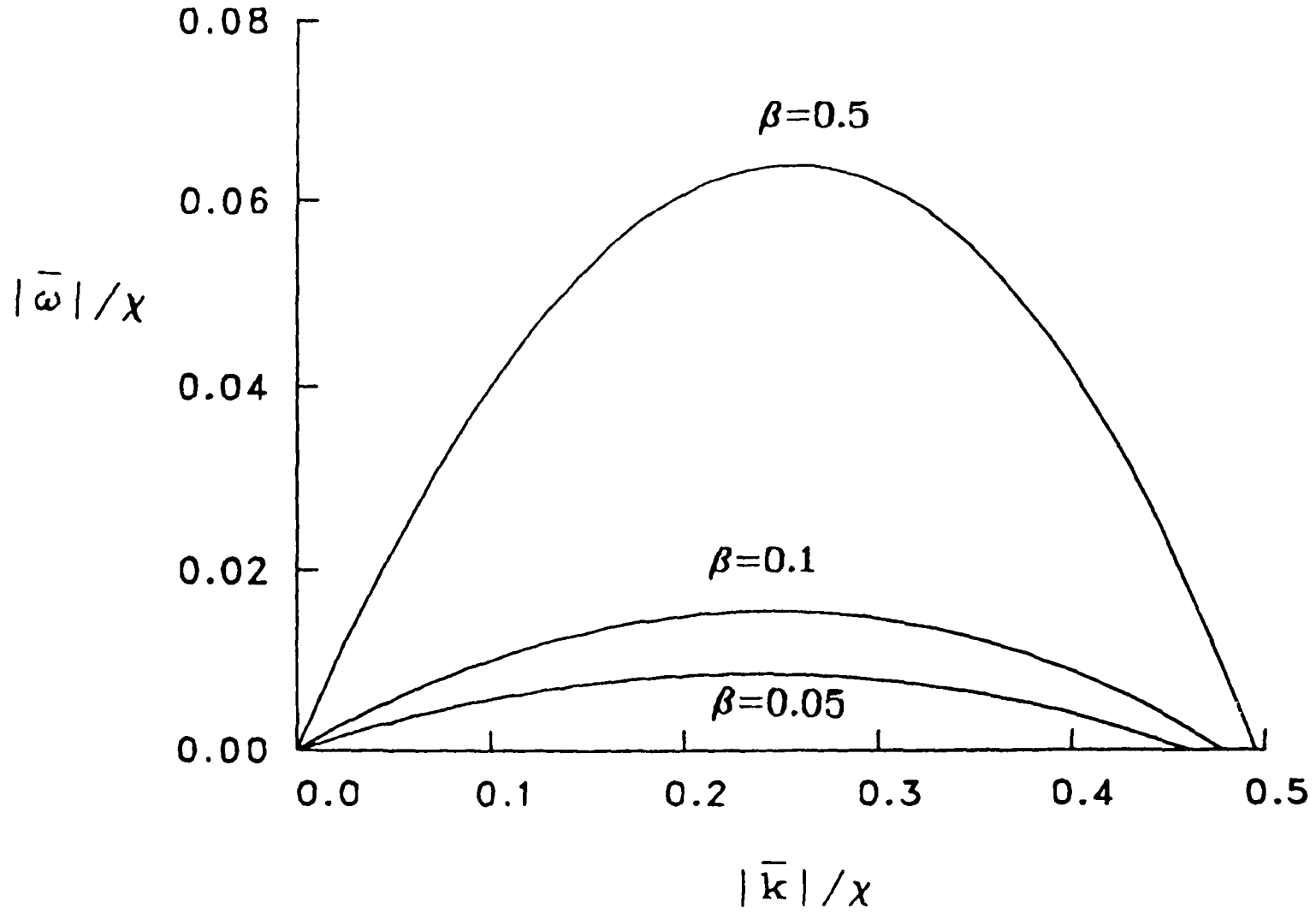

Figure 2. Dispersion curves for β = 0.05, 0.1, and 0.5. Respective values of χ are 0.073, 0.13, and 0.62.

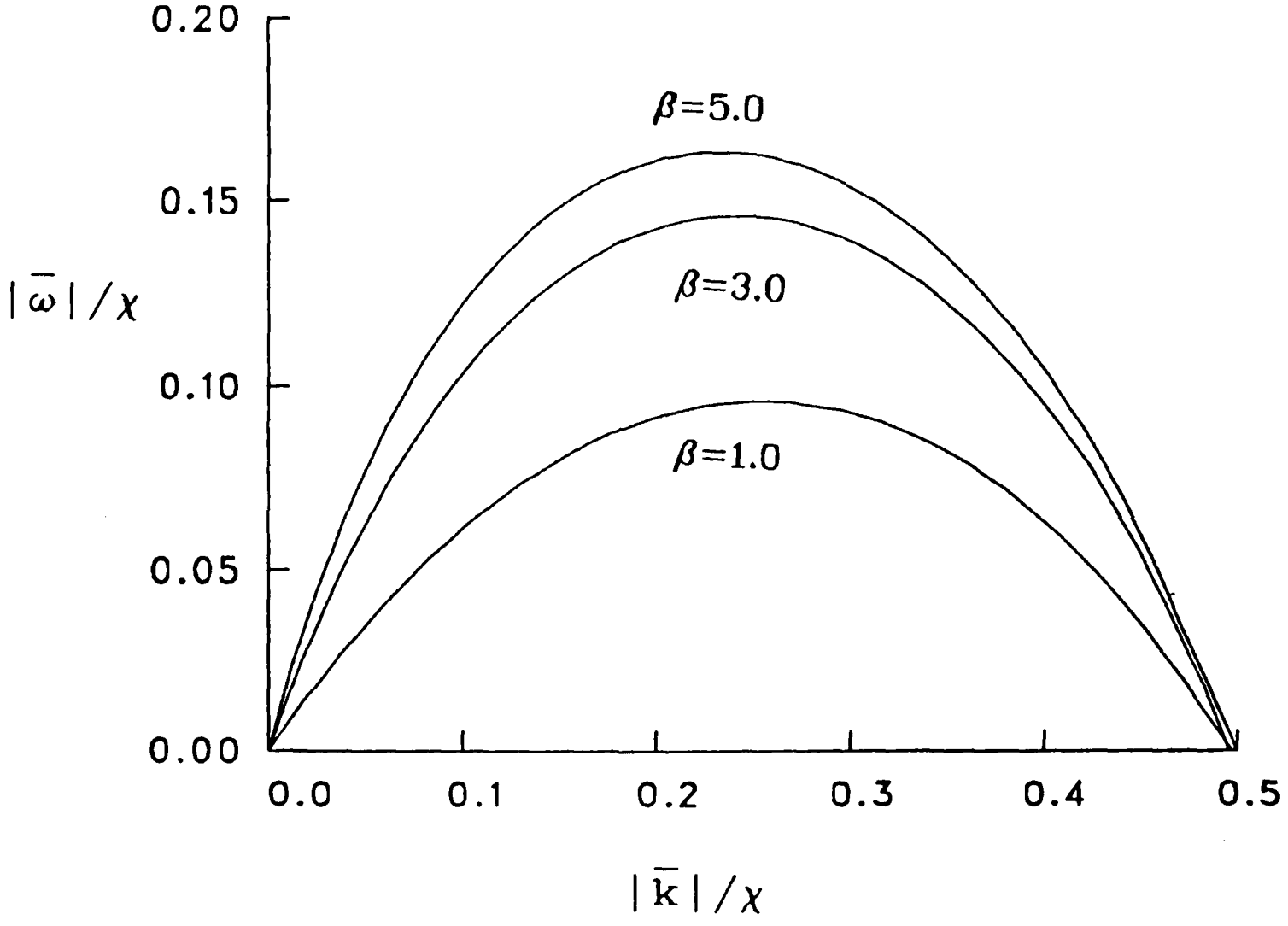

Figure 3. Dispersion curves for β = 1.0, 3.0, and 5.0. Respective values of χ are 1.08, 2.32, and 3.14.

IV. DISCUSSION

Our physical understanding of the dispersion curves in Figs. 2 and 3 can be described as follows. For the very-long-wavelength modes (small k), the perturbation is hardly felt in local regions of the plasma and the growth rate, which is proportional to ω, decreases with increasing wavelength. However, the deformation of the plasma with $\vec{k}$ parallel to $\vec{B}_0$ requires a bending of the lines of magnetic induction in order that the $\vec{B}$ field remain divergenceless. The bending of the lines is evident since $B_{1x} \neq 0$. The bent field lines now exert a stabilizing force on the plasma corresponding to an interaction of the unperturbed induction field with the component of the first-order current produced by B_{1x} [see the penultimate term on the right-hand side of Eq. (16)]. The strength of this stabilizing force increases as k increases and the lines become more severely bent. Thus, for sufficiently large k, this restoring force can counteract the destabilizing reaction force ($\rho_1 a_0$) and the plasma is stabilized. This situation should be compared to the interchange instability[1] in which the induction lines become stretched or compressed, but not bent, and ω continues to grow as k increases.

The instability produced by $\vec{k} \| \vec{B}_0$ is sometimes referred to as the current-filamentation instability. This descriptive title is applicable because the bent field lines tend to "squeeze off" or pinch areas of the plasma in which the current density will be high compared to that in the bulk of the gas. If the plasma is unstable the current density in these filaments will grow in time. The filamentary behavior is not possible without a bending of the induction lines since the formation of filaments clearly requires $\vec{J} \times \vec{B}$ forces in both Cartesian directions normal to the direction of current flow.

It is apparent from Figs. 2 and 3 that for values of $\beta \geq 0.5$ the plasma becomes stabilized at

$$\bar{k}_s / \chi \geq 0.5 \tag{41}$$

or

$$k_s = \frac{0.5 a_0}{K} \quad . \tag{42}$$

Consequently, for fixed K (or temperature) the destabilizing reaction force increases as a_0 increases and larger values of k are needed to produce stability. Alternatively, for fixed a_0, the arc length increases as T increases and the density at local points in the arc is reduced. Correspondingly, the reaction force is also reduced and stabilization can occur for smaller values of k. The same result indicated by Eq. (42) was found by TLW[2] for a plasma with conductivity proportional to the density, which was accelerated without a projectile, and which had infinitely extended tails.

For values of $\beta \leq 0.5$, the stability condition indicated in (42) becomes less severe as can be seen in Figs. 2 and 3. Perhaps the reason for the relaxation of the criterion at these small values of β is that stabilization occurs at wavelengths sufficiently long that size effects are important. In other words, these long-wavelength modes "see" that there is a fixed boundary at the projectile surface and the boundary exerts a stabilizing effect.[5] In general, the boundary becomes important for $k \ell_0 \leq 1$. It is a fairly simple exercise to show for the curves in Figs. 2 and 3 that $k_s \ell_0 < 1$ for values of $\beta \leq 1$, but not for larger values of β.

It is apparent that the maximum value of $\bar{\omega}$ occurs in each of the curves at points near $k_s/2$. We may write for these maxima

$$\frac{|\bar{\omega}_m|}{\chi} = C(\beta) \tag{43}$$

or

$$\omega_m = \frac{C(\beta) a_0}{\sqrt{R}} \tag{44}$$

where $C(\beta)$ appears to approach a numerical value of about 0.2 as β becomes large. That the maximum growth rate should increase with a_0, and decrease with K, is evident from previous discussion. Condition (44) should be compared with the maximum growth rate obtained by TLW, namely,

$$\omega_m = 0.2\, a_0/\sqrt{R} \quad . \tag{45}$$

It therefore appears that the growth rates of the instability for the constant-conductivity case are smaller than for the case worked out by TLW, particularly for small values of β. Undoubtedly, the greater stability is at least partly attributable to the finite-size effect discussed in reference to Eq. (42). A graph of $C(\beta)$ versus β is shown in Fig. 4 for the values of β indicated in Figs. 2 and 3, as well as for a few additional ones.

There remains the question of whether the instability is of any importance in railgun experiments. Evidently, rapidly accelerating, fairly cold, long arcs are the best candidates for demonstrating the effects of the instability, a set of conditions not easily achieved. As examples for discussion we have considered in Table I three sets of data. The first two correspond to actual experimental measurements on railguns; the last case is hypothetical as discussed.

[5] Kruskal, M.D. and Schwarzschild, M., *Proceedings of Plasma Physics* (McGraw-Hill, New York, 1957), Chap. 8.

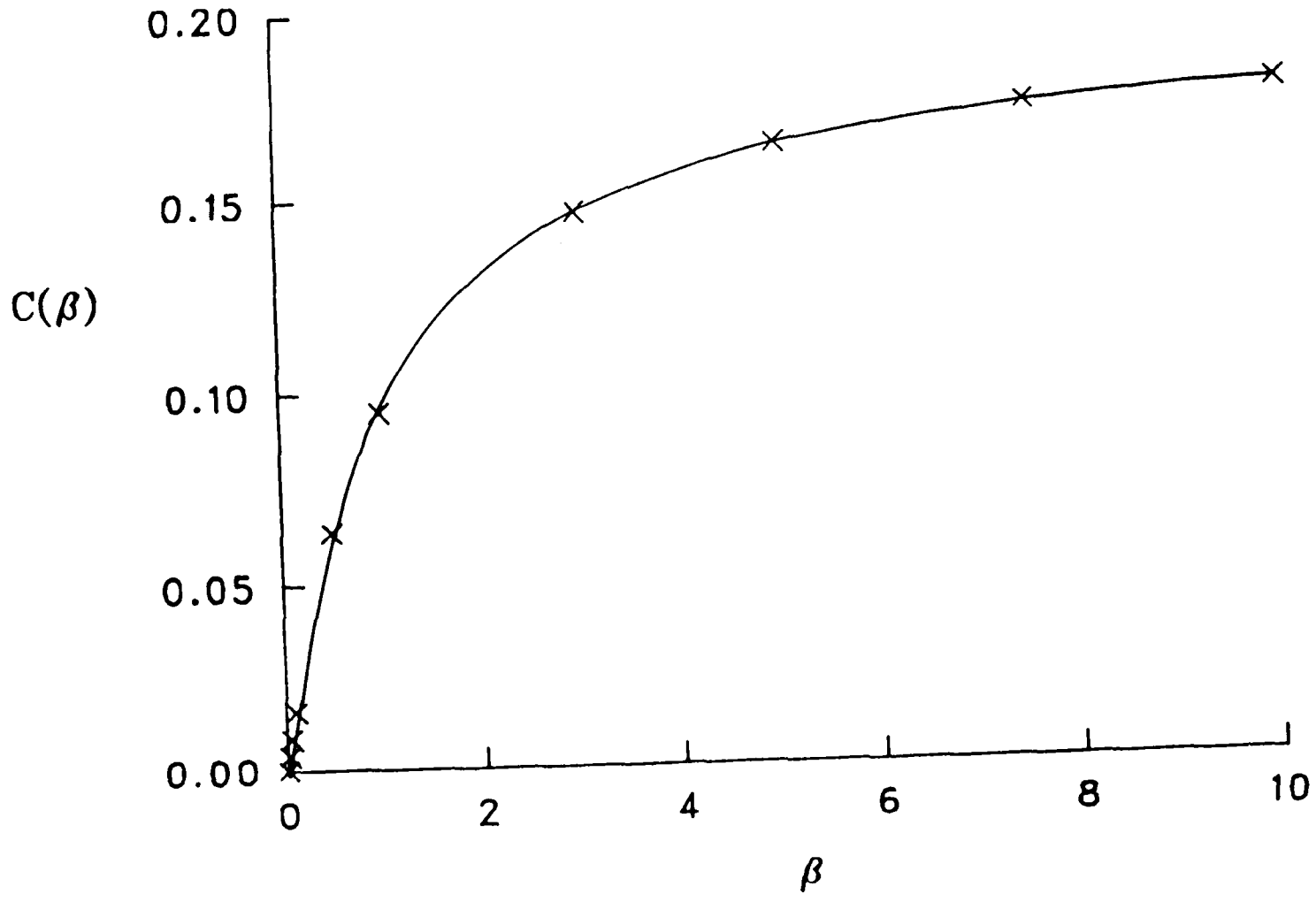

Figure 4. The parameter C(β) versus β [See Eq. (43)].

TABLE I. Data for Calculation of Stability Effects*

Case	a_0	ℓ_0	V_0	i	T	β	χ	$C(\beta)$	λ_s	t_e
I	7.2×10^5	0.044	180	100 kA	1.8×10^4 K	0.00195	0.0029	0.00033	189	14
II	1.1×10^6	0.30	310	800 kA	1.4×10^4 K	0.026	0.039	0.0044	97	0.59
III	2.3×10^7	0.72	-	800 kA	4.0×10^4 K	1.0	1.1	0.095	8.2	1.8 ms

*All units are MKS unless otherwise noted.

The first case in Table I corresponds to an experiment[6] carried out by Jamison and Burden on a small, one-half-inch, square-bore railgun at BRL. A 2.5 g projectile was accelerated using an aluminum arc ($M_0 \simeq 4.6 \times 10^{-26}$ kg) to about a kilometer per second. Measurements of a_0, ℓ_0, the current i, and the muzzle voltage V_0 were made at various points along the gun tube; the values indicated in the table were obtained at a point about 15 cm from the breech. The arc temperature was very roughly approximated by assuming that one-third of the measured muzzle voltage corresponded to a resistive drop across the plasma[7] and calculating the conductivity σ of the arc. The temperature was then inferred from the theoretical expression[3] for the Spitzer conductivity which gives σ as a function of T. The arc was assumed to be singly ionized. Once these parameters are known K, χ and β follow from Eqs. (6), (29) and (30), and C(β) can be obtained by interpolation using the data in Fig. 4. Finally, ω_m and k_s follow from Eqs. (44) and (42), and the e-folding time associated with the maximum growth rate as well as the stabilizing wavelength from the expressions

$$t_e = \frac{1}{\omega_m} \tag{46}$$

and

$$\lambda_s = 2\pi / k_s \quad . \tag{47}$$

The magnitude of the last two quantities indicates that the instability is utterly negligible in this experiment. Not only is the e-folding time orders of magnitude larger than the acceleration time, but also the wavelengths associated with the instability are large compared to the railgun dimensions in the z direction (not accounted for in the model).

The second case considered in Table I corresponds to diagnostic data recently taken by Jamison and Burden[5] on CHECMATE, the two-inch, square-bore railgun at Maxwell Laboratories. In this case an aluminum arc was used to accelerate a 100 g projectile. Values of ℓ_0, V_0, and i were again taken directly from the data, but the acceleration was calculated from the current and (assumed) inductance gradient of the railgun, namely, 0.4 μH/m. The temperature and remaining parameters were then calculated in a manner identical to that for Case I. Note that even though the arc is nearly an order of magnitude longer than before, the temperature smaller, and the acceleration nearly a factor of two larger, the instability is apparently still unimportant. In particular, both λ_s and t_e are still too large for the instability to have any practical importance.

---

[6] Jamison, K.A., Marshall-Felmet, M. and Burden, H.S., "Measurements of the Spatial Distributions of Current in a Rail Gun Arc Armature," IEEE Trans. Magn. MAG-20, 403 (1984).

[7] Powell, J.R., "Electromagnetic Mass Injection Acceleration by a High Pressure Plasma," J. Appl. Phys. 33, 1962 (1962).

[5] Jamison, K.A., Parker, J.V., Personal communication.

Finally, we consider a hypothetical case, similar to Case I, but for a longer arc and higher current. We choose the arc material to be copper ($M_0 \simeq 1.1 \times 10^{-25}$ kg), assume a current of 800 kA, a projectile mass of 2.5 g, and take $\beta = 1$. The temperature was approximated by scaling the value for Case I according to previously derived scaling relations.[9] The plasma was assumed to be doubly ionized here since the temperature turns out to be somewhat higher than in Case I. These parameters are then sufficient to specify the steady state of the arc, and the remaining variables in the table can be calculated as before. We did use the scaling relations to obtain the acceleration from Case I, rather than use Eq. (29), since this theoretical result is known to overestimate the acceleration substantially.[3,9] Obviously, now, the acceleration and arc length are enormous; indeed, it is doubtful that small railguns could withstand these large currents and very long railguns would be necessary to accelerate such long arcs. At any rate, the e-folding time t_e is sufficiently short that instability effects might be seen. However, λ_s is still too long to be allowed by any practical railgun.

In summary, it appears that the current-filamentation instability is of virtually no importance in railgun applications, at least whenever macroscopic projectiles are accelerated. Evidently, the wavelengths at which stabilization occurs are generally long compared to reasonable railgun dimensions, and the e-folding times are generally long compared to typical acceleration times. This conclusion should be contrasted with that for the interchange instability, in which the growth rates always increase with decreasing wavelength, and effects of the instability are always expected to be important in railgun applications.

Improvements in the present model are not likely to result in any change in the basic conclusion concerning the importance of the current-filamentation instability in railgun accelerators. Probably the greatest limitation of the model is the assumption of infinite conductivity in the dispersion calculations. A priori, however, one would expect that finite conductivity would reduce the growth rates even more. This conclusion appears to be consistent with recent work by Sloan[10] and by Huerta and Decker.[11] Sloan has carried out some limiting-case calculations and speculated that growth rates should decrease with decreasing conductivity. Huerta and Decker have included the effects of finite conductivity in the TLW model and worked out the interchange case explicitly. Although their work is apparently still underway, early results appear to be consistent with Sloan's speculation.

---

[9] Powell, John D. and Batteh, Jad H., "Two-Dimensional Plasma Model for the Arc-Initiated Rail Gun," J. Appl. Phys. 54, 2241 (1983). See also Powell, John D., "Two-Dimensional Model for Arc Dynamics in the Rail Gun," Ballistic Research Laboratory Report No. ARBRL-TR-02433, October 1982.

[10] Sloan, M.L., "Some Considerations of Rayleigh-Taylor Instability in Armature Plasmas," Kaman Research Associates Report No. I-AFA-86-U-FF, 1986.

[11] Huerta, A.V., and Decker, M.L., "Finite Conductivity and the Rayleigh-Taylor Interchange Instability," Proceedings of the First EM Gun Armature Workshop, [illegible], 1, 41. See also Decker, A.M., Ballistic Research Laboratory, [illegible].

REFERENCES

1. Powell, John D., "Interchange Instability in Railgun Arcs," Phys. Rev. A, 34, 3262 (1968). See also Ballistic Research Laboratory Report No. BRL-TR-2276, January 1987.

2. Tsai, W., Liskow, D., and Wilcox, T., "Rayleigh-Taylor Instabilities of an Accelerating Thin Plasma," Phys. Fluids 24, 1676 (1981).

3. Powell, John D. and Batteh, Jad H., "Plasma Dynamics of an Arc-Driven, Electromagnetic, Projectile Accelerator," J. Appl. Phys. 52, 2717 (1981). See also, "Plasma Dynamics of the Arc-Driven Rail Gun," Ballistic Research Laboratory Report No. ARBRL-TR-02267, September 1980.

4. Kruskal, M. and Schwartzschild, M., "Some Instabilities of a Completely Ionized Plasma," Proc. R. Soc. London Ser. A 223, 348 (1954).

5. Krall, N.A. and Trivelpiece, A.W., Principles of Plasma Physics (McGraw-Hill, New York, 1973), Chap. 5.

6. Jamison, K.A, Marquez-Reines, M. and Burden, H.S., "Measurements of the Spatial Distributions of Current in a Rail Gun Arc Armature," IEEE Trans. Magn. MAG-20, 403 (1984).

7. McNab, I.R., "Electromagnetic Macroparticle Acceleration by a High Pressure Plasma," J. Appl. Phys. 51, 2549 (1980).

8. Jamison, Keith A. (private communication).

9. Powell, John D. and Batteh, Jad H., "Two-Dimensional Plasma Model for the Arc-Driven Rail Gun," J. Appl. Phys. 54, 2242 (1982). See also Powell, John D., "Two-Dimensional Model for Arc Dynamics in the Rail Gun," Ballistic Research Laboratory Report No. ARBRL-TR-02423, October 1982.

10. Sloan, M.L., "Some Considerations of Rayleigh-Taylor Instability in Armature Plasmas," Austin Research Associates Report No. I-ARA-86-U-36, 1986.

11. Decker, A.M. and Huerta, M.A., "Finite Conductivity and the Rayleigh-Taylor Interchange Instability," Proceedings of the First EM Gun Armature Workshop, Eglin AFB, FL, June 1986, p. 458. See also Decker, A.M., Finite Conductivity and the Rayleigh-Taylor Interchange Instability, with Applications to Plasma Arcs in Electromagnetic Rail-Launch Devices, Ph.D. thesis, University of Miami, 1986.

DISTRIBUTION LIST

No. of Copies	Organization
2	Administrator Defense Technical Info Center ATTN: DTIC-FDAC Cameron Station, Bldg 5 Alexandria, VA 22304-6145
10	C.I.A. DIR/DB/Standard GE47 HQ Washington, DC 20505
1	HQDA ATTN: DAMA-ART-M Washington, DC 20310
1	Commander US Army Armament RD&E Center ATTN: SMCAR-MSI Dover, NJ 07801-5001
1	Commander US Army ARDEC ATTN: SMCAR-TDC Dover, NJ 07801
1	Commander US Army RD&E Center ATTN: SMCAR-SCA-E, Mr. H. Kahn Dover, NJ 07801-5001
2	Commander US Army RD&E Center ATTN: SMCAR-LCA-C Dr. G.L. Ferrentino Dr. Thaddeus Gora Dover, NJ 07801-5001
1	Commander US Army Materiel Command ATTN: AMCDRA-ST 5001 Eisenshower Avenue Alexandria, VA 22333-0001
2	Commander US AMCCOM ARDEC CCAC Benet Weapons Laboratory ATTN: SMCAR-CCB-TL SMCAR-LCB-DS Dr. C.A. Andrade Watervliet, NY 12189-4050
1	Commander US Army Armament, Munitions & Chemcial Command ATTN: AMSMC-IMP-L Rock Island, IL 61299-7300
1	Commander US Army Aviation Systems Command ATTN: AMSAV-ES 4300 Goodfellow Blvd St. Louis, MO 63120-1798
1	Director US Army Aviation Research & Technology Center Ames Research Center Moffett Field, CA 94035-1099
1	Commander US Army Communications - Electronics Command ATTN: AMSEL-ED Ft. Monmouth, NJ 07703-5301
1	Commander CECOM R&D Technical Library ATTN: AMSEL-IM-L, Reports Section B. 2700 Ft. Monmouth, NJ 07703-5000
1	Commander US Army Missile Command ATTN: AMSMI-R Redstone Arsenal, AL 35898

DISTRIBUTION LIST

No. of Copies	Organization
2	Director US Army Missile Command ATTN: AMSMI-YDL Redstone Arsenal, AL 35898-5500
1	Director Ballistic Missile Defense Advanced Technology Center ATTN: BMDATC-M, Dr. D.B. Harmon Huntsville, AL 35807
2	Director DARPA ATTN: Dr. Harry Fair Dr. Peter Kemmey 1400 Wilson Blvd Arlington, VA 22209
1	Commander US Army Tank Automotive Command ATTN: AMSTA-TSL Warren, MI 48397-5000
1	Commandant US Army Infantry School ATTN: ATSH-CD-CSL-OR Ft. Benning, GA 31905-5400
1	Commander US Army Development & Employment Agency ATTN: MODE-ORO Ft. Lewis, WA 98433-5000
5	Commander SDIO ATTN: SDIO/KEW, BG M. O'Neil MAJ R. Lennard SDIO/IST Dr. J. Ionson Dr. L. Caveny Washington, DC 20301-7100
1	Director US Army Research Office ATTN: Dr. Mikael Ciftan Research Triangle Park, NC 27709-2211
1	Commander Naval Surface Weapons Center ATTN: Mr. P.T. Adams, Code G-35 Dahlgren, VA 22448-5000
2	Commander Naval Research Laboratory ATTN: Dr. I.M. Vitkovitsky, Code 4701 Mr. R. Ford, Code 4474 Washington, DC 20375
1	AFWL/SUL Kirtland AFB, NM 87117
5	Air Force Armament Laboratory ATTN: AFATL/DLDODL ATATL/DLYS, CPT J. Brown LT J. Martin Mr. Kenneth Cobb LT D. Jensen Dr. Timothy Aden Eglin AFB, FL 32542-5000
1	AFAPL/POCS-2 ATTN: Dr. Charles E. Oberly Wright-Pattersen AFB Dayton, OH 45433
1	Director Brockhaven National Laboratory ATTN: Dr. J.R. Powell, Bldg 129 Upton, NY 11973
1	Director Lawrence Livermore National Lab ATTN: Dr. R.S. Hawke, L-156 FO Box 808 Livermore, CA 94550
3	Director Los Alamos National Laboratory ATTN: MSG 787, Mr. Max Fowler Dr. Gerry V. Parker Dr. Mark Parsons, MS D472 Los Alamos, NM 87545

DISTRIBUTION LIST

No. of Copies	Organization
1	Sandia National Laboratory ATTN: Dr. Maynard Cowan, Dept 1220 PO Box 5800 Albuquerque, NM 87185
1	NASA Lewis Research Center ATTN: Lynette Zana, MS 501-7 2100 Brook Park RD Cleveland, OH 44135
1	Astron Research & Engineering ATTN: Dr. Charles Powars 2028 Old Middlefield Way Mountain View, CA 94043
2	Austin Research Associates ATTN: Dr. Millard L. Sloan Dr. William E. Drummond 1091 Rutland Drive Austin, TX 87858
2	Maxwell Laboratories ATTN: Dr. Rolf Dethlefson Dr. Michael M. Holland 8888 Balboa Avenue San Diego, CA 92123
3	Electromagnetic Research Inc. ATTN: Dr. Henry Kolm Dr. Peter Mongeau Mr. William Snow 625 Putnam Avenue Cambridge, MA 62139
1	BDM Corporation ATTN: Dr. David Elkin 10260 Old Columbia RD Columbia, MD 21046
1	Boeing Aerospace Company ATTN: Dr. J.E. Shrader PO Box 3999 Seattle, WA 98134
2	GA Technologies, Inc. ATTN: Dr. Robert Bourque Dr. L. Holland PO Box 85608 San Diego, CA 92138
5	GT Devices ATTN: Dr. Derek Tidman Dr. Shyke Goldstein Dr. Neils Winsor Dr. Y.C. Thio Dr. Rodney L. Burton 5705-A General Washington Drive Alexandria, VA 22312
1	General Dynamics ATTN: Dr. Jaime Cuadros PO Box 2507 Pomona, CA 91766
1	General Electric Company ATTN: Dr. John Hickey, Bldg 37 Room 380 1 River RD Schnectady, NY 12345
3	General Electric Company (AEPD) ATTN: Dr. William Bird Dr. W. Condit Dr. Slade L. Carr RD#3, Plains RD Ballston Spa, NY 12020
1	General Research Corporation ATTN: Dr. William Isbell 5383 Hallister Avenue Santa Barbara, CA 93111
1	Gould Defense Systems, Inc. Ocean Systems Division ATTN: Dr. Donald M. McEligot One Corporate Place Newport Corporate Park Middletown, RI 02840

DISTRIBUTION LIST

No. of Copies	Organization
2	IAP Research, Inc. ATTN: Dr. John P. Barber Dr. David P. Bauer 2763 Culver Ave. Dayton, OH 45459-3723
1	LTV Aerospace & Defense Company ATTN: Dr. Michael M. Tower Dr. C.H. Haight, M/S TH-83 PO Box 65003 Dallas, TX 75265-0003
1	Pacific-Sierra Research Corp. ATTN: Dr. Gene E. McClellan 1401 Wilson Blvd Arlington, VA 22209
3	Physics International Company ATTN: Dr. A.L. Brooks Dr. Edward B. Goldman Dr. Frank Davies 2700 Merced Street San Leandro, CA 94577
1	R&D Associates ATTN: Dr. Peter Turchi PO Box 9695 Marina del Rey, CA 90291
1	Rockwell International Rocketdyne Division ATTN: Dr. Earl Deder, MS HB14 6633 Canoga Avenue Canoga Park, CA 91304
2	SAIC ATTN: Dr. Jad H. Batteh Mr. G. Rolader 1519 Johnson Ferry RD, Suite 300 Marietta, GA 30062
2	SAIC Plasma Physics Division ATTN: Dr. John Connally 1710 Goodrich Drive, T4 McLean, VA 22102
1	SAIC ATTN: Dr. Dan Barnes 206 Wild Basin RD, Suite 103 Austin, TX 78746
1	System Planning Corporation ATTN: Donald E. Shaw 1500 Wilson Blvd Arlington, VA 22209
1	Electromagnetic Applications, Inc. ATTN: Dr. Ronal W. Larson 12567 W. Cedar Drive, Suite 250 Lakewood, CO 80228-2091
1	Westinghouse Electric Corporation Marine Division ATTN: Dr. Dan Omry Dr. Ian R. McNab 401 E. Hendy Avenue Sunnyvale, CA 94088-3499
1	Westinghouse R&D Laboratory ATTN: Dr. Bruce Swanson 1310 Beulah RD Pittsburgh, PA 15233
2	Auburn University ATTN: Dr. Raymond F. Askew, Director, Leach Nuclear Science Center Dr. E.J. Clothiaux, Dept of Physics Alabama, 36849-3501
1	Texas Technical University Department of EE/Computer Science ATTN: Dr. M. Kristiansen Lubbock, TX 79409-4439
1	Tuskegee Institute Department of Mechanical Engng ATTN: Dr. Pradosh Ray Alabama 36088
1	University of Alabama in Huntsville School of Science & Engineering ATTN: Dr. C.H. Chan Huntsville, AL 35899

DISTRIBUTION LIST

No. of Copies	Organization
1	University of Miami ATTN: Dr. Manuel A. Huerta Physics Department PO Box 248046 Coral Gables, FL 33124
1	University of Tennessee Space Institute ATTN: Dr. Dennis Keefer Tullahoma, TN 37388-8897
2	University of Texas Center for Electromechanics Balcones Research Center ATTN: Mr. William Weldon Mr. Raymond Zaworka 10100 Burnet RD, Bldg 133 Austin, TX 78758

Aberdeen Proving Ground

Dir, USAMSAA
ATTN: AMXSY-D
AMXSY-MP, H. Cohen

Cdr, USATECOM
ATTN: AMSTE-SI-F

Cdr, AMCCOM
ATTN: SMCCR-RSP-A
SMCCR-MU
SMCCR-SPS-IL

The following is an internal distribution list for the manuscript entitled,

Current- Filamentation Instability in Railgun Arcs

, written by John D. Powell

.

NAME	DIVISION	NO. COPIES
Iris Keirn	TBD	1
Wilma Hubbard	TBD	1
Robert Bossoli	TBD	1
Henry Burden	TBD	1
Steve Cornelison	TBD	1
Joseph Correri	TBD	1
Arthur Gauss, Jr.	TBD	1
Clinton Hollandsworth	TBD	1
Keith Jamison	TBD	1
Laszlo Kecskes	TBD	1
Tom Kottke	TBD	1
Keith Mahan	TBD	1
Miguel Marquez-Reines	TBD	1
Andrus Niiler	TBD	1
Frederick Pierce	TBD	1
Anand Prakash	TBD	1
Charles Stumpfel	TBD	1
George Thomson	TBD	1
Phil Yunker	TBD	1
Alex Zielinski	TBD	1
Judy Temperley	SECAD	1
Denis Strenzwilk	SECAD	1
Bill Anderson	IBD	1
Walter Egerland	SECAD	1
Donald Eccleshall	TBD	1

USER EVALUATION SHEET/CHANGE OF ADDRESS

This Laboratory undertakes a continuing effort to improve the quality of the reports it publishes. Your comments/answers to the items/questions below will aid us in our efforts.

1. BRL Report Number_____ Date of Report_____

2. Date Report Received_____

3. Does this report satisfy a need? (Comment on purpose, related project, or other area of interest for which the report will be used.)_____

4. How specifically, is the report being used? (Information source, design data, procedure, source of ideas, etc.)_____

5. Has the information in this report led to any quantitative savings as far as man-hours or dollars saved, operating costs avoided or efficiencies achieved, etc? If so, please elaborate._____

6. General Comments. What do you think should be changed to improve future reports? (Indicate changes to organization, technical content, format, etc.)

CURRENT ADDRESS

Name

Organization

Address

City, State, Zip

7. If indicating a Change of Address or Address Correction, please provide the New or Correct Address in Block 6 above and the Old or Incorrect address below.

OLD ADDRESS

Name

Organization

Address

City, State, Zip

(Remove this sheet, fold as indicated, staple or tape closed, and mail.)

FOLD HERE

rector
Army Ballistic Research Laboratory
TN: DRXBR-OD-ST
erdeen Proving Ground, MD 21005-5066

NO POSTAGE
NECESSARY
IF MAILED
IN THE
UNITED STATES

OFFICIAL BUSINESS
ENALTY FOR PRIVATE USE, $300

BUSINESS REPLY MAIL
FIRST CLASS PERMIT NO 12062 WASHINGTON, DC
POSTAGE WILL BE PAID BY DEPARTMENT OF THE ARMY

Director
US Army Ballistic Research Laboratory
ATTN: DRXBR-OD-ST
Aberdeen Proving Ground, MD 21005-9989

FOLD HERE

END

10-87

DTIC